Supporting Information

Crown ether functionalization boosts CO_2 electroreduction to ethylene on copper-based MOFs

Xuan Zheng,[1, +] Siheng Yang,[1, +] Dingwen Chen,[1] Yuxuan Kong,[2] Tianhua Cui,[1] Xueli Zheng,[1] Haiyan Fu,[1] Weichao Xue,[1] Shuang Li,[2] Chong Cheng,[2] Hua Chen,[1] Ruixiang Li,[1, *] Jiaqi Xu[1, 3, *]

[1] Key Laboratory of Green Chemistry & Technology, Ministry of Education, College of Chemistry, Sichuan University, Chengdu, Sichuan 610064, P.R. China

[2] College of Polymer Science and Engineering, State Key Laboratory of Polymer Materials Engineering, Sichuan University, Chengdu, 610065, China

[3] Laboratory of Photonics and Interfaces, École Polytechnique Fédérale de Lausanne, 1015 Lausanne, Switzerland

[+]These authors contributed equally to this work.

Email: liruixiang@scu.edu.cn (R. Li); jqxu@scu.edu.cn, jiaqi.xu@epfl.ch, jq-xu@qq.com (J. Xu)

S1. Experimental details

Materials: Copper(II) sulfate pentahydrate ($Cu(NO_3)_2 \cdot 5H_2O$), 1,3,5-benzenetricarboxylic acid ($C_9H_6O_6$, H_3BTC), 1,4-dicarboxybenzene ($C_8H_6O_4$, H_2BDC), 2-aminoterephthalic acid ($C_8H_7NO_4$, $H_2BDC\text{-}NH_2$), 1,4-Diazabicyclo[2.2.2]octane (DABCO), N, N-dimethylformamide (DMF), acetic acid, potassium hydroxide (KOH), Sodium hydroxide (NaOH), Lithium hydroxide (LiOH), Cesium Hydroxide Monohydrate ($CsOH \cdot H_2O$), ethanol, and 5 wt% Nafion solution were purchased from Beijing Innochem Science & Technology co., LTD.

Synthesis of CuBTC: In a typical synthetic procedure, 182 mg of copper nitrate was dissolved in 10 mL of methanol to prepare solution A; 87.5 mg of H_3BTC was dissolved in 10 mL of methanol to prepare solution B. Solution A was added into solution B and stirred for 2 hours. A blue precipitate was then obtained by allowing the mixture to stand. After centrifugation, collect the precipitate, wash it twice with water and ethanol respectively, and then freeze-dry to obtain CuBTC.[1]

Synthesis of CuBDC: First, 28.9 mg of $Cu(NO_3)_2 \cdot 5H_2O$, 32.4 mg of H_2BDC, and 11.2 mg of DABCO were sequentially added to 40 ml of DMF and sonicated for 15 minutes to ensure complete dissolution. Subsequently, the resulting blue solution was transferred into a Teflon liner and stirred for 10 minutes. The mixture was then placed into a 50 mL stainless-steel autoclave and heated at 120 ºC for 12 hours. After centrifugation, collect the precipitate, wash it twice with water and ethanol respectively, and then freeze-dry to obtain CuBDC.[2]

Synthesis of CuBDC-NH_2: the procedures were same as those for CuBDC, except that 32.4 mg (0.2 mmol) of H_2BDC was replaced by 36.2 mg (0.2 mmol) of $H_2BDC\text{-}NH_2$.[2]

Characterization: XRD patterns were obtained by a Shimazu XRD-6100 with Cu Kα radiation (λ = 1.5418 Å). For Scanning electron microscopy (SEM), the morphology of the prepared precursors and final materials were observed by high-resolution FE-SEM (Hitachi S-4000 and S-4800). Raman spectra were measured on a RenishawRM3000 Micro-Raman system. TEM images were measured by JEOL-2010 TEM. X-ray photoelectron spectra (XPS) spectra were carried out on ESCALAB MKII with Al Kα (hυ = 1486.6 eV) as the excitation source. The binding energies in the XPS spectral analysis were corrected by referencing C 1s to 284.8 eV.

Preparation of working electrode: 10 mg of catalyst and 10 μL of 5% Nafion solution were dispersed in 1 mL of isopropanol. Then, 0.2 mL of the above dispersion was dropped onto a piece of gas diffusion layer (YLS-30T) and heated at 65 °C for 10 minutes to dry the dispersion. To obtain electrodes with added crown ether, different masses of crown ether were added to the above dispersion, with all other steps remaining unchanged.

Electrocatalytic CO_2 reduction tests: All electrocatalytic tests and reactions were conducted using a CHI760E electrochemical workstation in a three-electrode system. And all the electrochemical measurements were conducted in a flow cell, separated by a Nafion membrane, with Hg/HgO (with saturated KOH as the filing solution) as the reference electrode and a 1 cm × 1 cm Ni foam as the counter electrode. Both the cathode and anode used 1M KOH solution as the electrolyte during the test. LSV was carried out in 1 M KOH solution at a scan rate of 50 mV s^{-1}. Electrochemical impedance spectroscopy (ElS) was conducted at open-circuit potential from 0.01 Hz to 100 kHz with an amplitude of 5 mV. The electrochemical active surface area (ECSA, cm^2) was calculated by double-layer capacitance C_{DL}, which was measured by conducting CV within a 100 mV window centered at -0.45 V vs. RHE. All potentials were eventually transformed to the reversible hydrogen electrode reference through the following relationship:

$$E_{vs\ RHE} = E_{vs\ Hg/HgO} + 0.098\ V + 0.0591\ V \times pH$$

Product analysis: The liquid products and gas products were qualitatively and quantitatively analyzed using nuclear magnetic resonance (NMR, AVIII400 HD) and gas chromatography (GC, PANNA GC-A60), respectively. The GC is equipped with two detectors: a thermal conductivity detector (TCD) and a flame ionization detector (FID).

For gas analysis, N_2 was used as the carrier gas for TCD to detect H_2, while FID was employed to detect CO, CH_4, and C_2H_4. The Faradaic efficiency (FE) of the products can be quantified following this formula,

$$FE_i = \frac{z_i \cdot n_i \cdot F}{Q_{total}} \times 100\ \%$$

z_i: The number of electrons involved in the reaction. n_i: The number of moles of the product. F: The Faraday constant, representing the charge per mole of electrons, F = 96485 $C \cdot mol^{-1}$. The mole amount of liquid product directly measured by ^1H NMR spectra, the volume of total electrolyte and the volume of the tested electrolyte, respectively.

In-situ ATR-FTIR measurement: A three-electrode configuration was used, with a carbon rod as the counter electrode and a saturated Hg/HgO as the reference electrode. The working electrode was prepared through dropping catalyst ink onto the silicon deposited with a gold film. The catholyte was 1.0 M KOH. Spectra were collected in situ under open circuit potential (OCP) and at different electrolysis steps with CO_2 introduced. This approach enabled real-time monitoring of the material's structural changes and reaction intermediates during the CO_2 electrochemical reduction processes.

S2. Supplementary characterizations

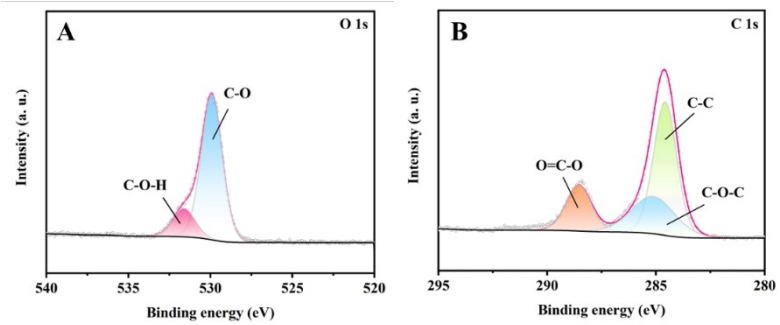

Figure S1. XPS survey spectrum for O 1s (A) and C 1s (B) of CuBTC. These signals primarily originate from the skeletal structure of H_3BTC in CuBTC.

As shown in the **Figure S1**, the signals of O 1s and C 1s in CuBTC both originate from the framework of H_3BTC.

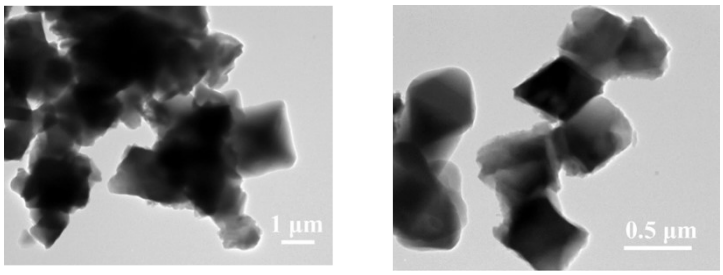

Figure S2. TEM images of CuBTC.

TEM images revealed the octahedral structure of CuBTC.[8]

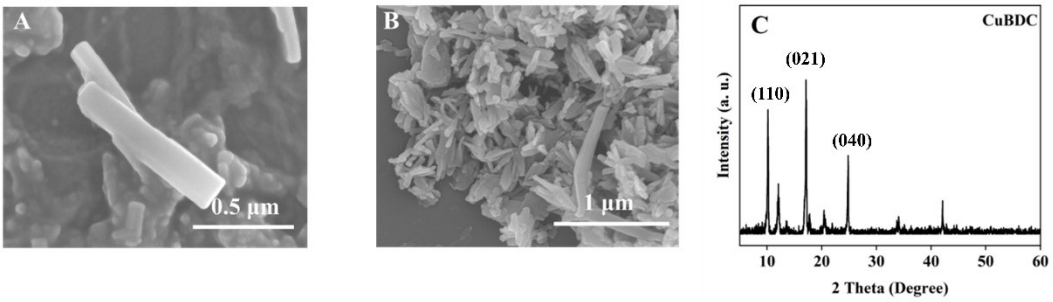

Figure S3. (A, B) SEM images of CuBDC. (C) The diffraction pattern of Cu-BDC.

A rod-like structure was observed for Cu-BDC, with a length of approximately 1 μm. The characteristic diffraction patterns at 2 theta = 10.2°, 17.2°, and 24.6° correspond to the (110), (021), and (040) planes of Cu-BDC, respectively.[3–7]

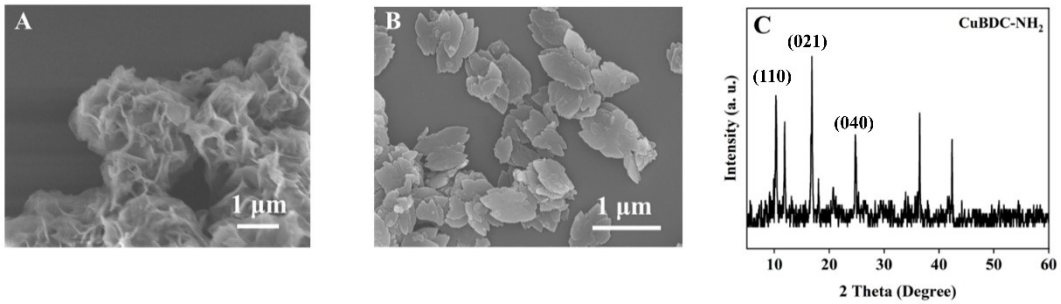

Figure S4. (A, B) SEM images of CuBDC-NH_2. (C) The XRD pattern of CuBDC-NH_2.

A sheet-like structure is clearly observed, and similar diffraction patterns to those of CuBDC are also present for CuBDC-NH_2. However, due to the modification with amino groups on the linker, several additional peaks appear.[4]

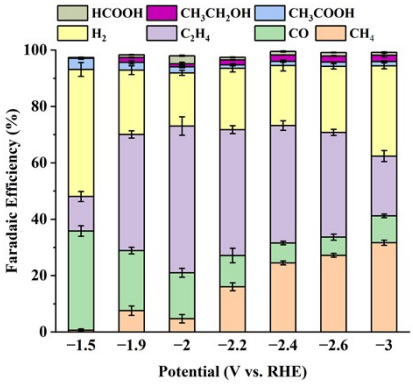

Figure S5. Distribution of ECO_2RR products on 2 mg cm^{-2} crown ether (CE)-modified CuBTC under different applied potentials.

Under these conditions, as the voltage increases, the ethylene yield first increases and then decreases, reaching its maximum value (ca. 52%) at -2.0 V vs. RHE.

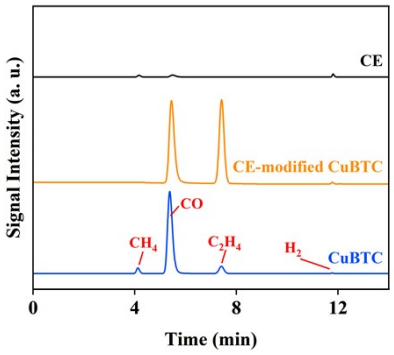

Figure S6. Typical gas chromatography profiles of CE, CuBTC, and CE-modified CuBTC during the ECO_2RR tests.

In the blank experiment with only CE added, apart from trace impurity gases (CH_4, CO) originating from the CO_2 gas itself, only an H_2 signal was detected. This can be attributed to the gas diffusion layer (GDL), which tends to generate hydrogen under electrochemical conditions. Under the same experimental conditions, CuBTC primarily produces CO as the main product. However, with the addition of crown ether, a strong ethylene signal peak is observed. This indicates the addition of CE promote the formation of ethylene.

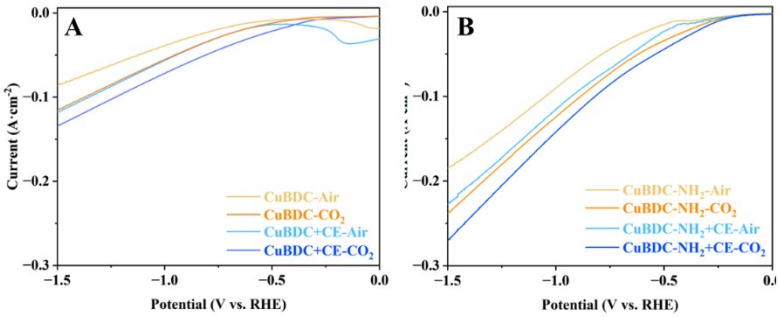

Figure S7. (A) Linear sweep voltammetry curves of CuBDC; (B) Linear sweep voltammetry curves of CuBDC-NH_2.

As shown in **Figure S7A**, the current under a CO_2 atmosphere is higher compared to that under air conditions, indicating higher activity toward CO_2. This current further increases after the addition of CE. A similar situation can also be observed in **Figure S7B**.

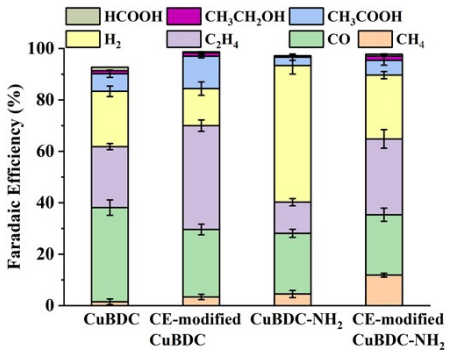

Figure S8. Distribution of ECO_2RR products for CuBDC and CuBDC-NH_2 with and without CE addition.

Compared to the pure catalyst, the addition of CE significantly enhances the FE of ethylene for CuBDC and CuBDC-NH_2.

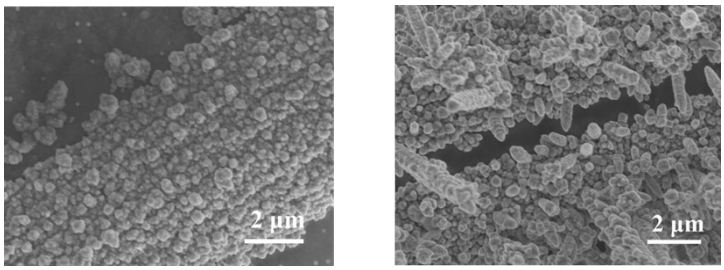

Figure S9. SEM images of CuBTC loaded on carbon paper after ECO_2RR.

The octahedral structure of CuBTC is observed to collapse and undergo in-situ reconstruction into a particle-assembled rod-like structure, suggesting that the active species changes during the ECO_2RR process.

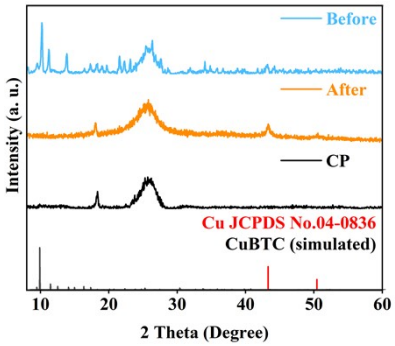

Figure S10. The XRD diffraction patterns of pure CuBTC on carbon paper before and after the ECO_2RR.

Before the reaction, the diffraction patterns are mainly attributed to CuBTC and carbon paper (CP). After the ECO_2RR, the diffraction patterns shift to those corresponding to Cu and CP, indicating that, without CE modification, the crystal phase of the catalyst transforms into metallic copper.

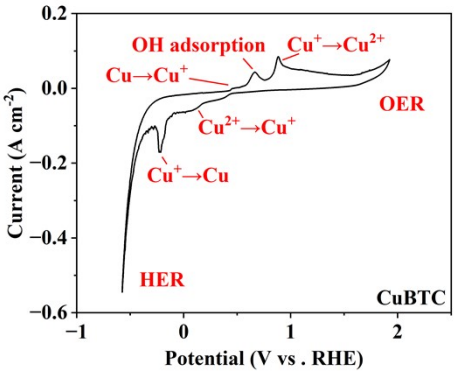

Figure S11. Cyclic voltammetry (CV) curve of pure CuBTC after the ECO_2RR.

As shown in the **Figure S11**, two pairs of redox couples are clearly observed in the CV curve of pure CuBTC, corresponding to Cu^{2+}/Cu^{+} and Cu^{+}/Cu. This indicates that CuBTC can be transformed into metallic Cu without CE-modification.

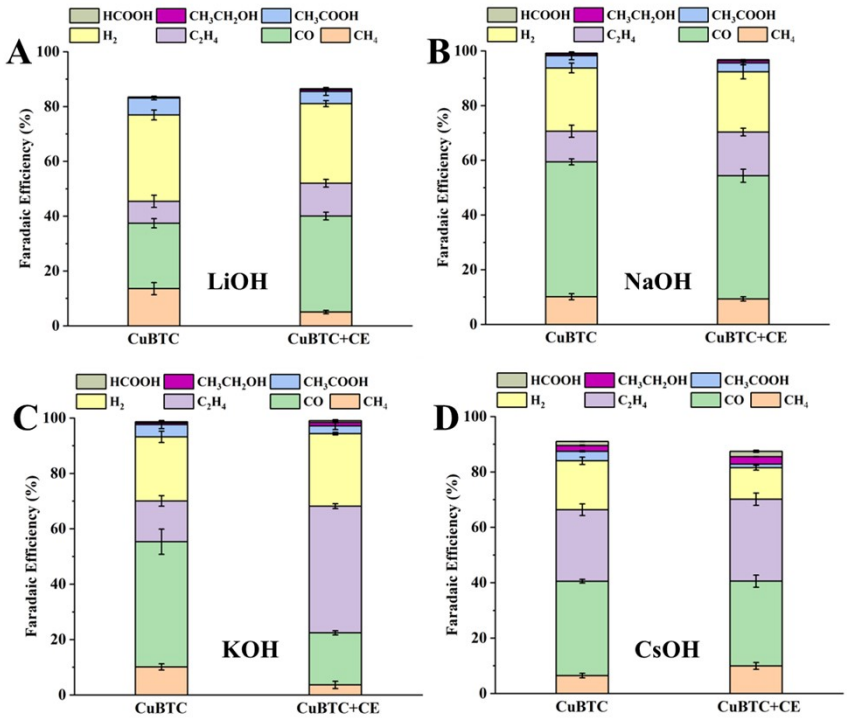

Figure S12. (A) Distribution of ECO_2RR products for CuBTC with and without the addition of CE in 1 M LiOH. (B) Distribution of ECO_2RR products for CuBTC with and without the addition of CE in 1 M NaOH. (C) Distribution of ECO_2RR products for CuBTC with and without the addition of CE in 1 M KOH. (D) Distribution of ECO_2RR products for CuBTC with and without the addition of CE in 1 M CsOH.

In **Figure S12** unlike in KOH, the addition of CE does not significantly increase ethylene selectivity for CuBTC in LiOH, NaOH, and CsOH.

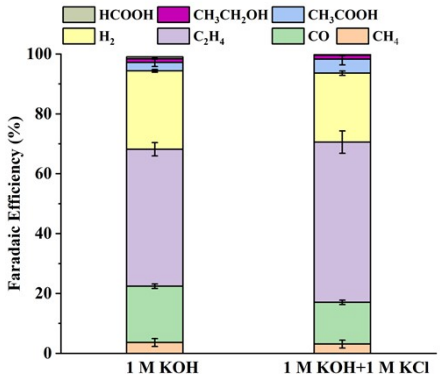

Figure S13. Comparison of ECO_2RR products distribution for CE-modified CuBTC with and without additional potassium ion.

As shown in **Figure 13**, the addition of 1 M KCl to the KOH solution further enhances the ethylene selectivity of CE-modified CuBTC catalyst.

Reference

(1) Zang, Y.; Liu, T.; Wei, P.; Li, H.; Wang, Q.; Wang, G.; Bao, X. Selective CO_2 Electroreduction to Ethanol over a Carbon-Coated CuO_x Catalyst. *Angew. Chem. Int. Ed.* **2022**, *61* (40), e202209629. https://doi.org/10.1002/anie.202209629.

(2) Chen, R.; Cheng, L.; Liu, J.; Wang, Y.; Ge, W.; Xiao, C.; Jiang, H.; Li, Y.; Li, C. Toward High-Performance CO_2 -to-C_2 Electroreduction via Linker Tuning on MOF-Derived Catalysts. *Small* **2022**, *18* (18), 2200720. https://doi.org/10.1002/smll.202200720.

(3) Silva, B. C. E.; Irikura, K.; Flor, J. B. S.; Dos Santos, R. M. M.; Lachgar, A.; Frem, R. C. G.; Zanoni, M. V. B. Electrochemical Preparation of Cu/Cu_2O-Cu(BDC) Metal-Organic Framework Electrodes for Photoelectrocatalytic Reduction of CO_2. *J. CO_2 Util.* **2020**, *42*, 101299. https://doi.org/10.1016/j.jcou.2020.101299.

(4) Zhan, G.; Fan, L.; Zhao, F.; Huang, Z.; Chen, B.; Yang, X.; Zhou, S. Fabrication of Ultrathin 2D Cu-BDC Nanosheets and the Derived Integrated MOF Nanocomposites. *Adv Funct Mater* **2019**, *29*, 1806720. https://doi.org/10.1002/adfm.201806720.

(5) Zhang, Q.; Chen, M.; Zhong, L.; Ye, Q.; Jiang, S.; Huang, Z. Highly Effective Removal of Metal Cyanide Complexes and Recovery of Palladium Using Quaternary-Ammonium-Functionalized MOFs. *Molecules* **2018**, *23* (8), 2086. https://doi.org/10.3390/molecules23082086.

(6) Khoshakhlagh, A. H.; Golbabaei, F.; Beygzadeh, M.; Carrasco-Marín, F.; Shahtaheri, S. J. Toluene Adsorption on Porous Cu–BDC@OAC Composite at Various Operating Conditions: Optimization by Response Surface Methodology. *RSC Adv.* **2020**, *10* (58), 35582–35596. https://doi.org/10.1039/D0RA06578A.

(7) Chen, R.; Cheng, L.; Liu, J.; Wang, Y.; Ge, W.; Xiao, C.; Jiang, H.; Li, Y.; Li, C. Toward High-Performance CO_2 -to-C_2 Electroreduction via Linker Tuning on MOF-Derived Catalysts. *Small* **2022**, *18* (18), 2200720. https://doi.org/10.1002/smll.202200720.

(8) Zhang, L.; Peng, L.; Lu, Y.; Ming, X.; Sun, Y.; Xu, X.; Xia, Y.; Pang, K.; Fang, W.; Huang, N.; Xu, Z.; Ying, Y.; Liu, Y.; Fu, Y.; Gao, C. Sub-Second Ultrafast yet Programmable Wet-Chemical Synthesis. *Nat. Commun.* **2023**, *14* (1), 5015. https://doi.org/10.1038/s41467-023-40737-5.